

# Data Visualization

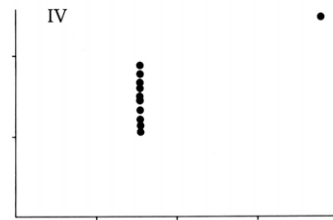
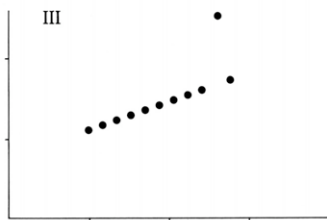
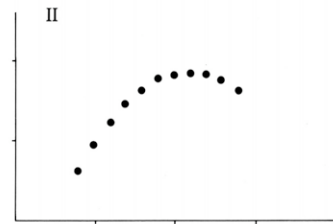
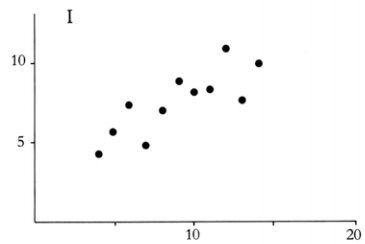
Steve Marschner

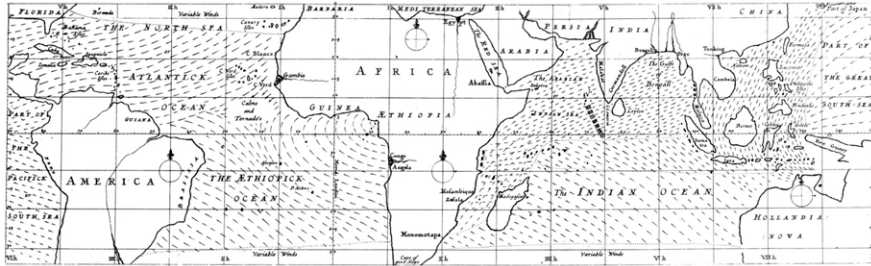
Cornell CS 322

unless noted, images are from our supplementary textbook:  
 Tufte, *The Visual Display of Quantitative Information*

I		II		III		IV	
X	Y	X	Y	X	Y	X	Y
10.0	8.04	10.0	9.14	10.0	7.46	8.0	6.58
8.0	6.95	8.0	8.14	8.0	6.77	8.0	5.76
13.0	7.58	13.0	8.74	13.0	12.74	8.0	7.71
9.0	8.81	9.0	8.77	9.0	7.11	8.0	8.84
11.0	8.33	11.0	9.26	11.0	7.81	8.0	8.47
14.0	9.96	14.0	8.10	14.0	8.84	8.0	7.04
6.0	7.24	6.0	6.13	6.0	6.08	8.0	5.25
4.0	4.26	4.0	3.10	4.0	5.39	19.0	12.50
12.0	10.84	12.0	9.13	12.0	8.15	8.0	5.56
7.0	4.82	7.0	7.26	7.0	6.42	8.0	7.91
5.0	5.68	5.0	4.74	5.0	5.73	8.0	6.89

$N = 11$   
 mean of X's = 9.0  
 mean of Y's = 7.5  
 equation of regression line:  $Y = 3 + 0.5X$   
 standard error of estimate of slope = 0.118  
 $t = 4.24$   
 sum of squares  $X - \bar{X} = 110.0$   
 regression sum of squares = 27.50  
 residual sum of squares of Y = 13.75  
 correlation coefficient = .82  
 $r^2 = .67$





E. Halley. Map illustrating trade winds. 1686





[NASA]

Space Shuttle mission STS-51-L, about 75 sec. after liftoff. 1986

HISTORY OF O-RING DAMAGE ON SRM FIELD JOINTS

SRM No.	Cross Sectional View			Top View		Clocking Location (deg)
	Erosion Depth (in.)	Perimeter Affected (deg)	Nominal Dia. (in.)	Length Of Max Erosion (in.)	Total Heat Affected Length (in.)	
61A LH Center Field**	22A	NONE	NONE	0.280	NONE	36° - 56°
61A LH Forward Field**	22A	NONE	NONE	0.280	NONE	338° - 18°
51C LH Forward Field**	15A	0.010	154.0	0.280	4.25	163
51C RH Center Field (prim)***	15B	0.038	130.0	0.280	12.50	58.75
51C RH Center Field (sec)***	15B	NONE	45.0	0.280	NONE	29.50
41D RH Forward Field	13B	0.028	110.0	0.280	3.00	NONE
41C LH Aft Field*	11A	NONE	NONE	0.280	NONE	--
41B LH Forward Field	10A	0.040	217.0	0.280	3.00	14.50
STS-2 RH Aft Field	2B	0.053	116.0	0.280	--	90

\*Hot gas path detected in putty. Indication of heat on O-ring, but no damage.  
 \*\*Soot behind primary O-ring.  
 \*\*\*Soot behind primary O-ring, heat affected secondary O-ring.  
 Clocking location of leak check port - 0 deg.

OTHER SRM-15 FIELD JOINTS HAD NO BLOWHOLES IN PUTTY AND NO SOOT NEAR OR BEYOND THE PRIMARY O-RING.

SRM-22 FORWARD FIELD JOINT HAD PUTTY PATH TO PRIMARY O-RING, BUT NO O-RING EROSION AND NO SOOT BLOWBY. OTHER SRM-22 FIELD JOINTS HAD NO BLOWHOLES IN PUTTY.

data presented by rocket's manufacturer to argue for canceling the launch.

*BLOW BY HISTORY*  
 SRM-15 WORST BLOW-BY  
 o 2 CASE JOINTS (80°), (110°) ARC  
 o MUCH WORSE VISUALLY THAN SRM-22

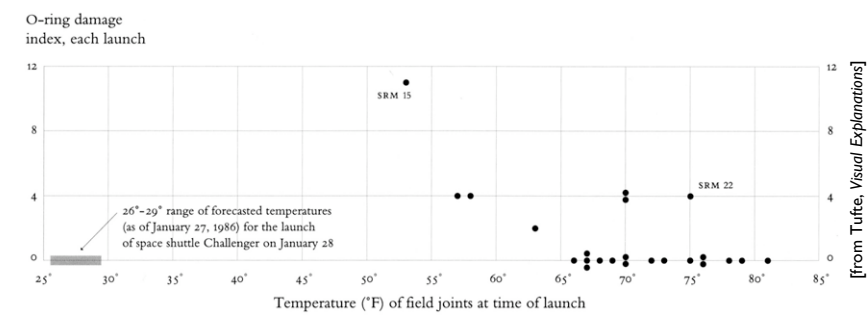
*SRM 22 BLOW-BY*  
 o 2 CASE JOINTS (30-40°)

*SRM-13A, 15, 16A, 18, 23A 24A*  
 o NOZZLE BLOW-BY

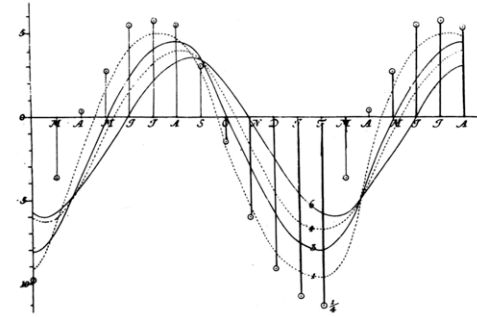
HISTORY OF O-RING TEMPERATURES (DEGREES - F)

MOTOR	MGT	A.M.B.	O-RING	WIND
DM-1	68	36	47	10 MPH
DM-2	76	45	52	10 MPH
QM-3	72.5	40	48	10 MPH
QM-4	76	48	51	10 MPH
SRM-15	52	64	53	10 MPH
SRM-22	77	78	75	10 MPH
SRM-25	55	26	29	10 MPH
			27	25 MPH

data presented by rocket's manufacturer to argue for canceling the launch.

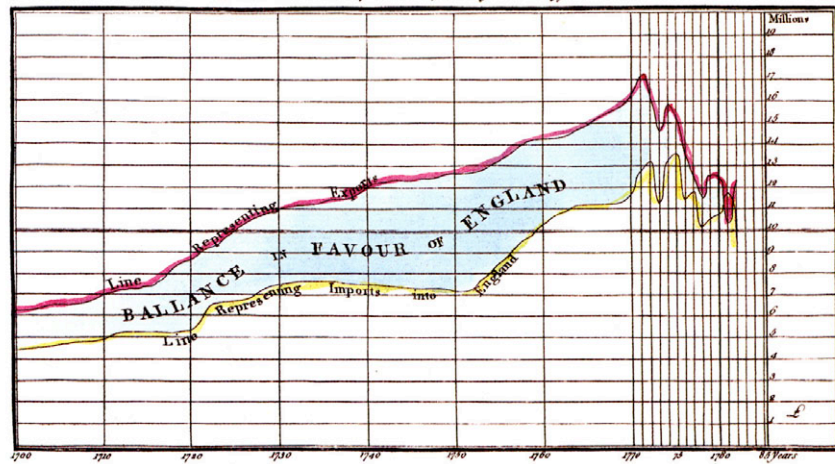


Tufte's more convincing re-presentation of the same data. 1997

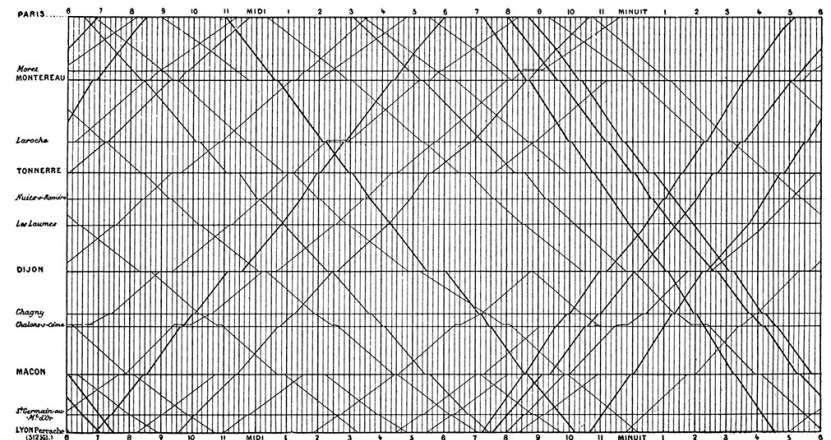


J.H. Lambert. Soil temperature over time at various depths. 1779

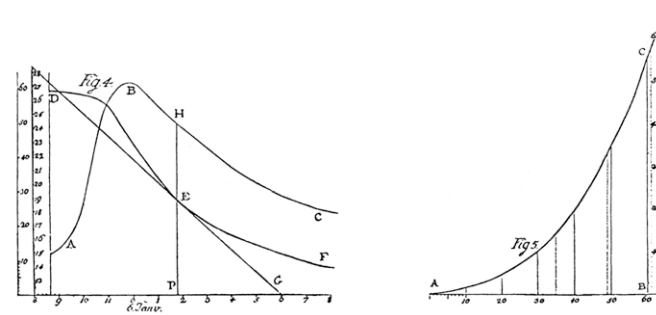
*CHART of all the IMPORTS and EXPORTS to and from ENGLAND From the Year 1700 to 1782 by W. Playfair*



*The Divisions at the Bottom, express YEARS, & those on the Right hand, MILLIONS of POUNDS  
J. Smith Sculp. Published as the Act directs, 20<sup>th</sup> Aug<sup>r</sup> 1788*



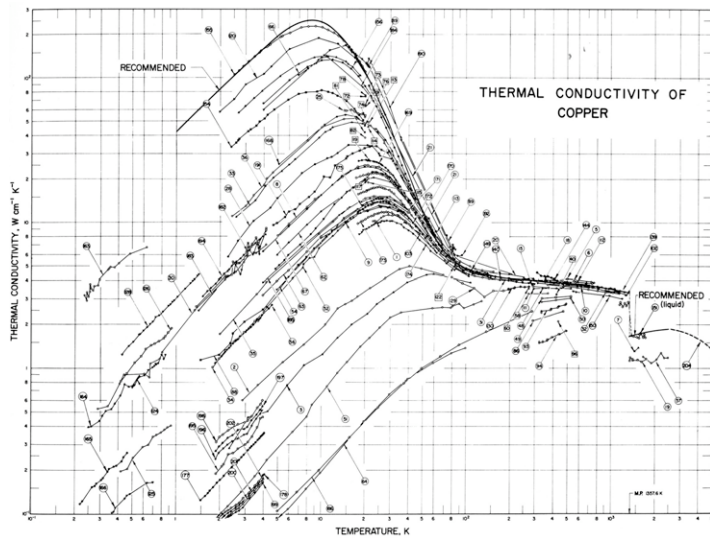
E.J. Marey. Train schedule for Paris-Lyon line. 1885



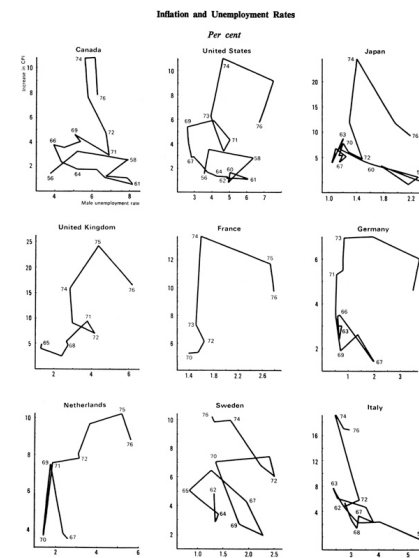
ABC: temperature over time  
DEF: height of water over time

evaporation rate  
vs. temperature

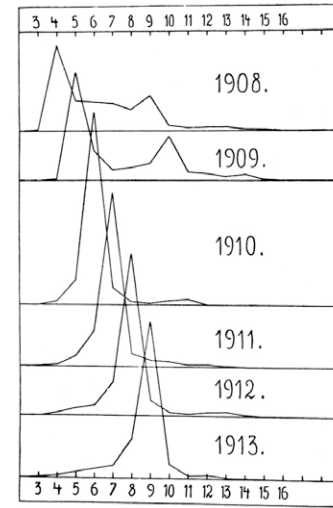
J.H. Lambert: influence of temperature on evaporation. 1769



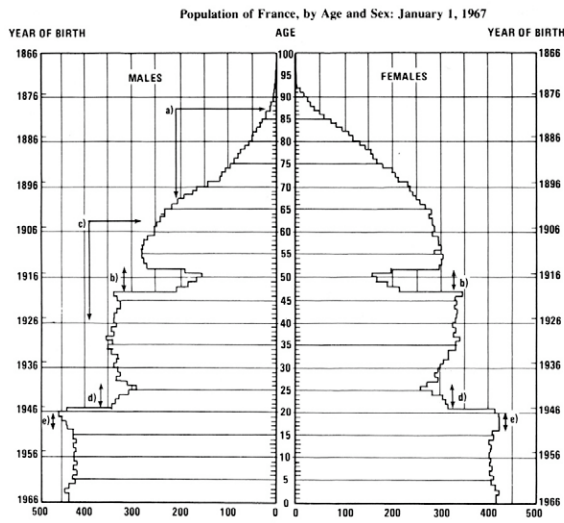
C.Y. Ho et al. Review of thermal conductivity data. 1974



P. McCracken et al. Phillips curves. 1977



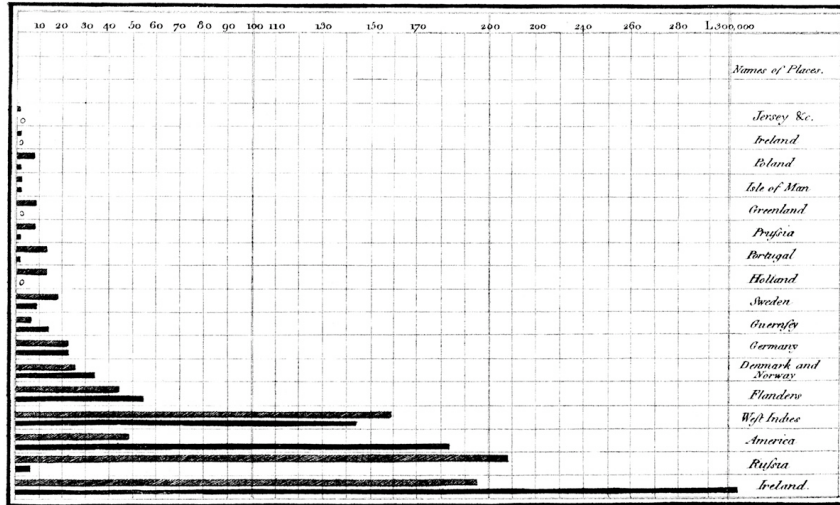
J. Hjort. Age composition of herring catches. 1914



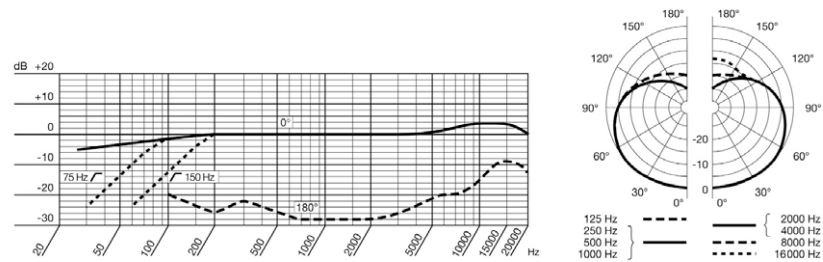
- (a) Military losses in World War I
- (b) Deficit of births during World War I
- (c) Military losses in World War II
- (d) Deficit of births during World War II
- (e) Rise of births due to demobilization after World War I

H.S. Shyrock & J.S. Siegel. Rendering of French government population data. 1973

Exports and Imports of SCOTLAND to and from different parts for one Year from Christmas 1780 to Christmas 1781

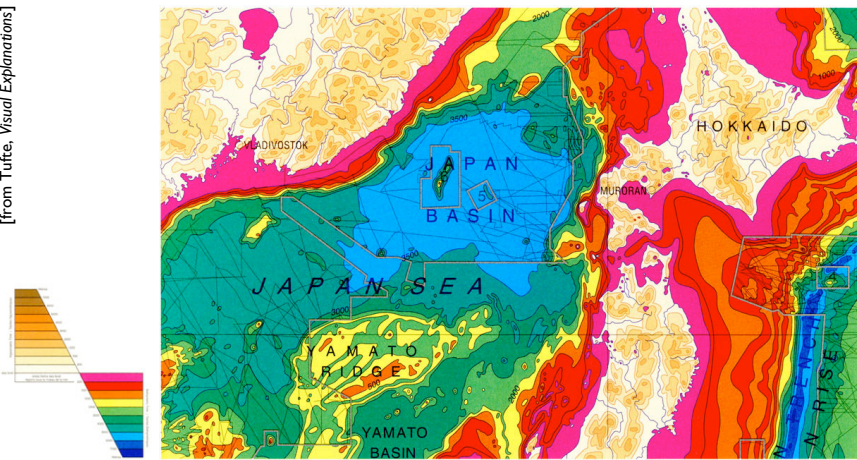


The Upright divisions are Ten Thousand Pounds each. The Black Lines are Exports the Ribbed lines Imports  
 Published in the Act-Decca, June 7<sup>th</sup> 1781 by W<sup>m</sup> Playfair  
 Made engr<sup>r</sup> J. S. S. Strand, London.



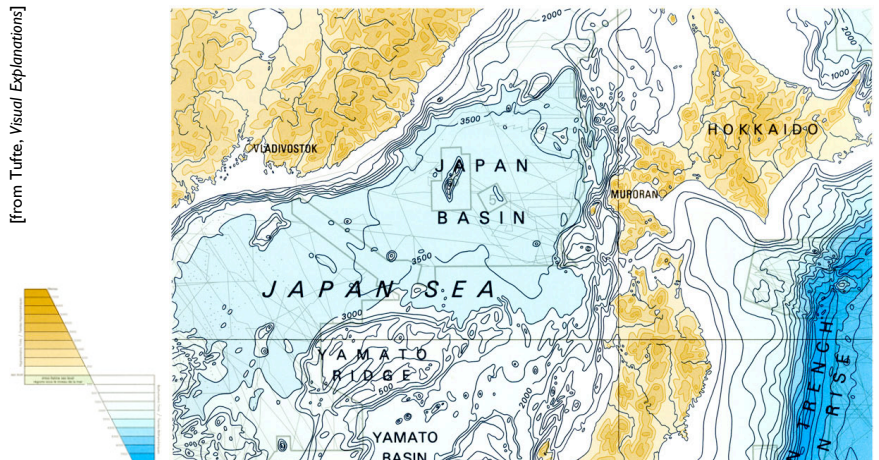
AKG Acoustics. Performance data for C451B microphone. 1973

[from Tufte, Visual Explanations]

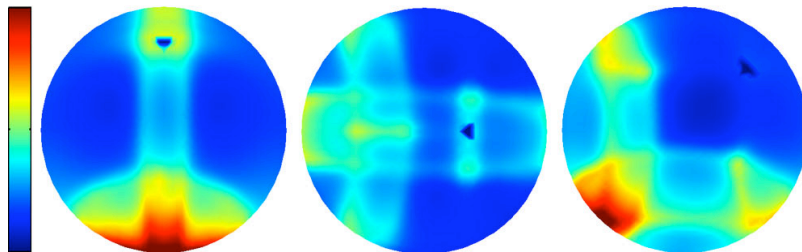


International Hydrographic Organization, 1984  
(as deliberately corrupted by Tufte)

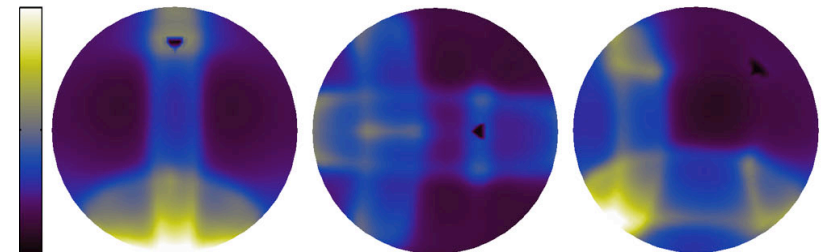
[from Tufte, Visual Explanations]



International Hydrographic Organization, 1984

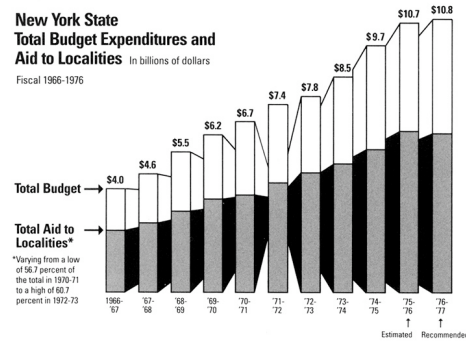


P. Irawan & S. Marschner. Scattering data for polyester cloth. 2007  
(Matlab default colormap)

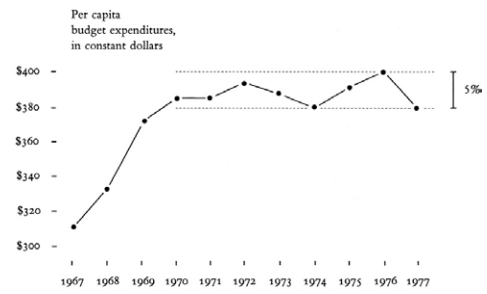


P. Irawan & S. Marschner. Scattering data for polyester cloth. 2007  
(increasing value colormap)

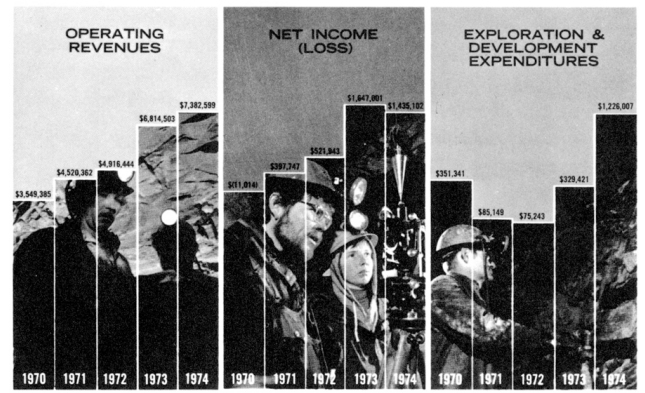




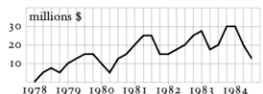
New York Times, 1976



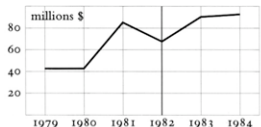
E. R. Tufte. Fair presentation of the same data. 1983



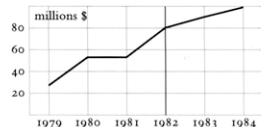
Day Mines, Inc. 1974



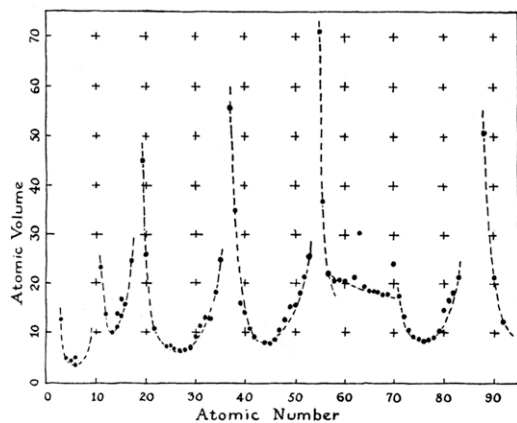
Above, this chart shows *quarterly* revenue data in a financial graphic for a legal case. Several dips in revenue are visible.



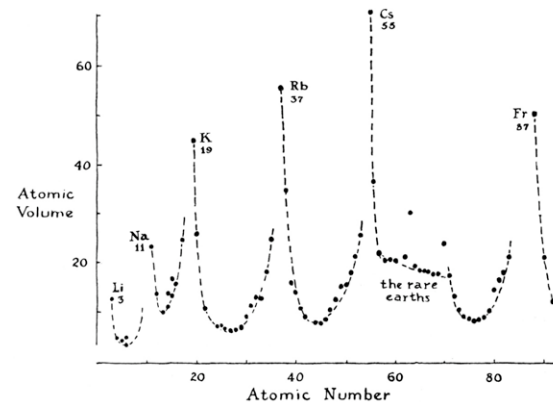
Aggregating the quarterly data into years, this chart above shows revenue by *fiscal year* (beginning July 1, ending June 30). Note the dip in 1982, the basis of a claim for damages.



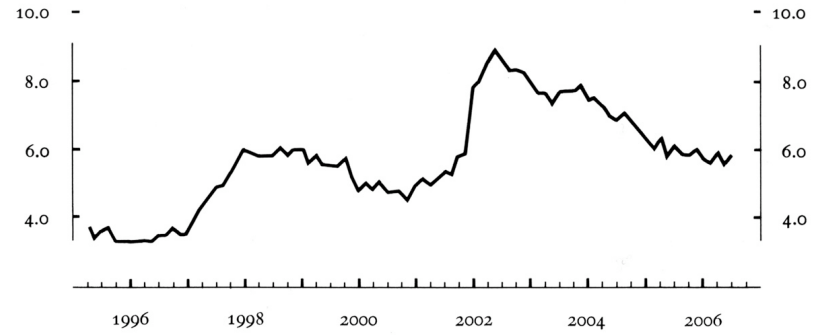
Shown above are the same quarterly revenue data added up into *calendar years*. The 1982 dip has vanished.



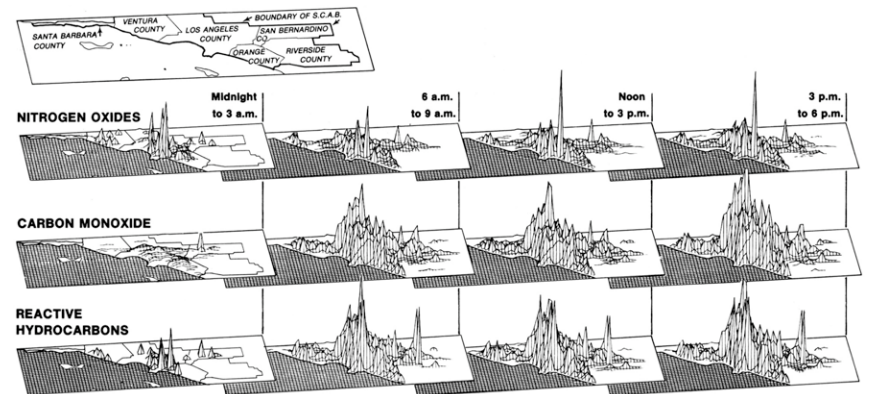
R. Hayward. From L. Pauling, *General Chemistry*. 1947



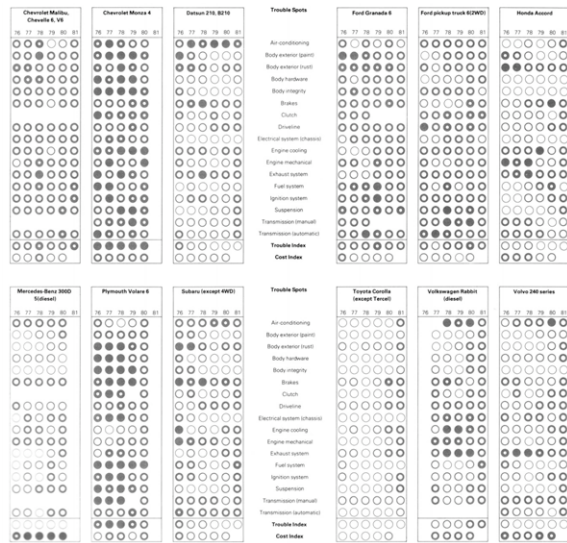
as modified by Tufte



Tufte's proposal for range frames



Los Angeles Times / G.J. McRae. 1979



Consumer Reports. Display of historical automobile reliability data. 1982

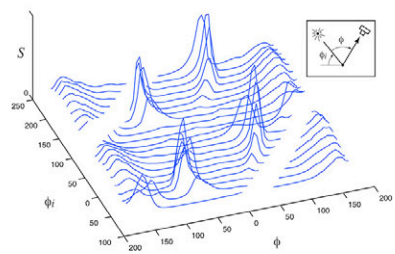


Figure 6: A measurement of scattering in the normal plane from a hair with substantial eccentricity. Bright glints appear whose location and strength depend on the orientation of the hair [subject HM].

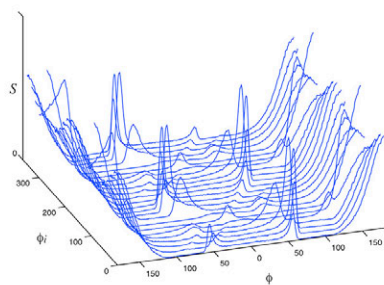
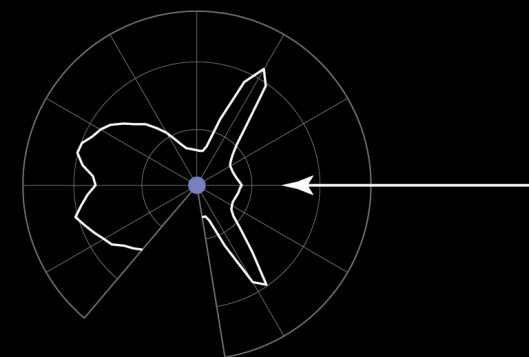


Figure 7: A photon-tracing simulation of scattering from a rough elliptical fiber. The axes are the same as in Figure 6.

S.R. Marschner. Presentation of fiber scattering data using default MATLAB plots. 2002



S.R. Marschner. Re-presentation using polar coordinates and small multiples. 2003  
(thanks to François Guimbretière)  
Marschner, Jensen, Cammarano, Worley, and Hanrahan. "Light Scattering from Human Hair Fibers," SIGGRAPH 2003.

